A conservative nonlinear filter for the high-frequency range of wind wave spectra ☆

Hendrik L. Tolman *

NOAA/NCEP/EMC, Marine Modeling and Analysis Branch, 5200 Auth Road, Room 209, Camp Springs, MD 20746, USA

ABSTRACT

Filtering of the high-frequency part of a wind wave spectrum may be useful in a numerical wind wave model for various reasons. First, it can be used to augment (or be part of) a parameterization of the resonant nonlinear interactions, that are essential to third-generation wind wave models. Second, when combined with a dynamic time stepping scheme for source term integration, it may result in smoother (and hence faster) wave model integration. In this study, such a filter is proposed, based on the traditional Discrete Interaction Approximation (DIA) for the resonant four-wave nonlinear interactions. This filter retains all conservative properties of the interactions. For small time steps and/or smooth spectra, it is formulated as a traditional source term. For larger time steps and/or non-smooth spectra it is formulated as a filter. This formulation guarantees stability of the filter itself and will enhance overall computational stability in a full wave model. The stability properties of this filter are illustrated using traditional wave growth computations. Examples are given where the filter improves model economy, and where it is shown to remove spurious high-frequency noise from a wave model.

Published by Elsevier Ltd.

1. Introduction

Wind waves at sea represent a stochastic process. The characteristics of such waves are generally described using wave energy or variance spectra, based on the original work with radio waves of Rice (1944). Typically such a spectrum is described in terms of frequencies f and directions θ associated with spectral wave components. Away from the surf zone, the phase information of spectral components is generally ignored resulting in a random-phase approach, and only the spectral energy level is considered. The evolution of the spectral energy is described or modeled using a spectral balance equation (Hasselmann, 1960), which in its simplest form becomes

$$\frac{DF(f,\theta)}{Dt} = S_{in}(f,\theta) + S_{nl}(f,\theta) + S_{ds}(f,\theta), \qquad (1)$$

where $F(f,\theta)$ is the energy or variance spectrum, S_{in} is a source term describing wind-wave interactions (wind input), S_{nl} describes nonlinear interactions between wave components in the spectrum, and S_{ds} describes wave dissipation, typically associated with wave breaking or 'whitecapping'. The left side of this equation describes (conservative) linear wave propagation.

The nonlinear interactions S_{nl} describe third-order resonant nonlinear interactions between four wave components. It is critical in describing wave growth, as these resonant interactions are generally believed to be the lowest order processes able to shift energy to lower frequencies (longer waves) at arbitrary depth, and to result in uniform spectral shapes at high frequencies (e.g., Hasselmann et al., 1973). In third-generation wave models, defined as models where spectral shapes are determined by the explicit source term balance, rather than by resorting to pre-described spectral shapes and energy levels, the parameterization of nonlinear interactions is of paramount importance. Such a third-generation approach to wind wave modeling is believed to be essential for accurate general-purpose wind wave models (SWAMP group, 1985).

Explicitly computing (the balance of) all source terms up to high frequencies introduces complications in numerical wind wave models. First, time scales of spectral change at high frequencies become small, resulting in prohibitively small numerical time steps if the time evolution of the corresponding spectral components is to be resolved. In many operational wave models a simple solution to avoid computations with excessively small time scales is to apply a parametric spectral shape ("tail") to frequencies above typically 3 times the spectral peak frequency (f_p) as associated with a growing wind sea. However, small time scales also occur in the frequencies $f_p < f < 3f_p$. Fortunately, source terms in this frequency ranges generally are in near-equilibrium conditions. This property is explicitly used in common time integration schemes for source terms in third-generations wave models (e.g., WAMDIG, 1988; Tolman, 1992; Hargreaves and Annan, 1998, 2001), allowing for economically acceptable numerical time steps. Another numerical acceleration technique is based on the introduction of so-called limiters, restricting the discrete change of energy per time step

per discrete spectral bin. Note that some limiters result in non-convergent model behavior (e.g., Hersbach and Janssen, 1999; Hersbach and Janssen, 2001; Tolman, 2002), and are therefore economically useful, but numerically suspect. Such limiters operate on individual spectral bins, and hence are non-conservative by nature.

Second, full computations of S_{nl} are prohibitively expensive for operational wave models, and economical yet accurate parameterizations have been elusive (Section 2). At least part of the problem with developing economical parameterizations of S_{nl} is that both large and small spectral-space scales of the exact interactions are important in describing wave growth. Interactions at larger spectral scales enable the (slow) evolution of the spectrum toward longer and higher waves, whereas small scale interactions are needed to stabilize the spectral shape at higher frequencies toward the local equilibrium solution (e.g., Young and Van Vledder, 1993). Many parameterizations have been suggested based on the large scale features of the nonlinear interactions, but almost without exceptions such parameterizations do not result in viable numerical models since the small-scale interactions are not represented adequately. Only a highly simplified discrete analog to the full interactions (DIA, Hasselmann et al., 1985) has been proven adequate for use in numerical models. After 25 years, the DIA with minor modifications is still the only interaction parameterization used in operational wave models. The only approach that could be considered an exception to this is the SRIAM method used in Japan (e.g., Tamura et al., 2008).

Both issues with numerical model integration at high frequencies are related to obtaining a near-equilibrium spectral solution at frequencies above the spectral peak frequency with numerical time steps that are larger than the evolutionary time scales involved. Ideally this can be achieved with a robust integration scheme designed to find near-equilibrium solutions (e.g., Hargreaves and Annan, 1998; Hargreaves and Annan, 2001), combined with a parameterization of S_{nl} that adequately describes the return to equilibrium solutions of a perturbed spectrum, as described in, e.g., Young and Van Vledder (1993). Present third generation models provide such an environment using the DIA, in spite of its many shortcomings (e.g., Van Vledder et al., 2000). Other proposed parameterizations of S_{nl}, however, are only partially successful in creating a dynamic source term balance at higher frequencies. Models using such parameterizations might benefit from filtering techniques that remove high-frequency noise from the resulting spectra. Due to the dominant role of the nonlinear interactions in stabilizing spectral shapes for frequencies above the spectral peak, it appears prudent for such a filter to have conservation and equilibrium properties of the nonlinear interactions. Such a filter is developed in the present study. It is shown that the traditional DIA can be reduced to a local quasi-diffusion. This reduced version of the DIA can be used as a source term that converts to a filter for large (economically feasible) time steps. It effectively adds a separate DIA configuration to a limited part of the spectral space, and is applied outside the general source term integration of a model. It is shown to reduce noise and accelerate model integration in a model using a Neural Network approximation to the interactions, and is shown to remove spurious high-frequency noise and increase model accuracy in some Generalized Multiple DIA configurations used to model nonlinear interactions.

Section 2 discusses nonlinear interactions and their parameterizations as relevant for the present study. In Section 3 the source term and filter is derived, and its parameter settings are assessed in the context of full wave growth in Section 4. In Section 5 the filter is applied to several practical wave modeling problems to show its potential impact. A discussion and conclusions are presented in Section 6.

2. Nonlinear interactions

The exact computation of the nonlinear interactions S_{nl} involves the evaluation of a six-dimensional Boltzmann integral. It includes an interaction function with strong moving singularities (e.g., Webb, 1978; Herterich and Hasselmann, 1980), and delta functions with contributions only for resonant sets of four wave components (so-called quadruplets), satisfying (Hasselmann, 1962, 1963)

$$\boldsymbol{k}_1 + \boldsymbol{k}_2 = \boldsymbol{k}_3 + \boldsymbol{k}_4, \tag{2}$$

$$\sigma_1 + \sigma_2 = \sigma_3 + \sigma_4. \tag{3}$$

where $\boldsymbol{k}$ represent wavenumber vectors, and σ represents the corresponding intrinsic frequencies, related in the (deep water) dispersion relation

$$\sigma^2 = gk. \tag{4}$$

This effectively reduces the integral to a three-dimensional integral over spectral space. Even with present day computers, and with various improvements in the efficiency of the computation of these integrals (e.g., Masuda, 1980; Tracy and Resio, 1982; Resio and Perrie, 1991; Komatsu and Masuda, 1996; Van Vledder, 2000; Van Vledder, 2006) the exact integral is prohibitively expensive for use in practical models. When numerical packages for exact computations (e.g., Van Vledder, 2000; Van Vledder, 2006) are applied in commonly used wave models, they increase model run times typically by up to three orders of magnitude.

So far, only one cheap approximation to the nonlinear interactions has been proven suitable for incorporation in operational wave models. This is the Discrete Interaction Approximation (DIA) of Hasselmann et al. (1985). In this approximation, a single representative resonant quadruplet is considered, satisfying

$$\left.\begin{aligned} \boldsymbol{k}_2 &= \boldsymbol{k}_1 \\ \sigma_3 &= (1+\lambda)\sigma_1 \end{aligned}\right\}, \tag{5}$$

where λ is a constant, typically $\lambda = 0.25$, and where contributions to the interactions for the quadruplet components $\delta S_{nl,i}$ at $\boldsymbol{k}_i$ are computed as

$$\begin{pmatrix} \delta S_{nl,1} \\ \delta S_{nl,3} \\ \delta S_{nl,4} \end{pmatrix} = \begin{pmatrix} -2 \\ 1 \\ 1 \end{pmatrix} Cg^{-4} f_1^{11} \left[F_1^2 \left(\frac{F_3}{(1+\lambda)^4} + \frac{F_4}{(1-\lambda)^4} \right) - \frac{2F_1 F_3 F_4}{(1-\lambda^2)^4} \right], \tag{6}$$

where $F_i = F(f_i, \theta_i)$, and C is a constant, typically $C = 3 \times 10^7$. This expression is evaluated for $\boldsymbol{k}_i$ equivalent to each discrete spectral grid point, after which the total interaction is obtained by summation of all discrete contributions δS_{nl}. Note that $\boldsymbol{k}_3$ and $\boldsymbol{k}_4$ generally do not coincide with the discrete spectral grid, so that F_3 and F_4 need to be evaluated by bi-linear interpolation. Likewise, $\delta S_{nl,3}$ and $\delta S_{nl,4}$ need to be distributed over surrounding discrete spectral grid points, consistent with the bi-linear interpolation of F_3 and F_4. Implicit to Eq. (6) is the assumption of a logarithmic discrete frequency grid

$$f_{i+1} = X_f f_i, \tag{7}$$

where typically $X_f = 1.10$ for operational wave models and $X_f = 1.07$ for research models using the exact Boltzmann integral. Eq. (6) is based on a discrete equivalent to the full integration integral, and retains the conservation of energy, action and momentum implicit to the interactions, as long as the quadruplet satisfies the resonance conditions (Webb, 1978). Note that the interpolations of F, and distribution of δS_{nl} retain the conservation of these three quantities (e.g., Tolman, 2008, Section 2.2).

The DIA has been highly successful in making third-generation wave models feasible. However, it has also long been known to

include serious errors (e.g., Hasselmann et al., 1985; Van Vledder et al., 2000). Some progress has been made in improving the DIA, but this is outside the scope of the present study. Alternatively, diffusion approaches have been proposed as alternative parameterizations for S_{nl} (e.g., Hasselmann et al., 1985; Zakharov and Pushkarev, 1999; Jenkins and Phillips, 2001). Whereas these methods do not appear to be able to produce desired model accuracies by themselves, they are of interest for the present study since diffusion operators provide a natural starting point for the development of filters.

3. A DIA-based filter

The filter developed here uses the similarity between the structure of nonlinear interaction contributions in the DIA, and a conventional discrete implementation of a simple diffusion equation. To this end, the traditional diffusion equation is discussed first. For an arbitrary parameter A evolving in time t and space x this equation is given as

$$\frac{\partial A}{\partial t} - D\frac{\partial^2 A}{\partial x^2} = 0, \tag{8}$$

where D is the diffusion coefficient. In a traditional forward-time-central-space finite difference approach, the numerical solution to this equation becomes

$$A_j^{n+1} = A_j^n + s\left(A_{j-1}^n - 2A_j^n + A_{j+1}^n\right), \quad s = \frac{D\Delta t}{(\Delta x)^2}, \tag{9}$$

where j and n are discrete space and time counters, and Δx and Δt are discrete space and time increments, respectively. Stability requires that the discretization parameter s is limited as (e.g., Fletcher, 1988, Section 7.1.1)

$$s \leqslant 0.5, \tag{10}$$

which is typically achieved by limiting Δt accordingly. Eq. (9) can also be interpreted as a smoothing algorithm. If the diffusion coefficient D varies in space, a conservative version of Eq. (9) can be obtained if the algorithm is implemented as a redistribution rather than averaging algorithm. For the grid point j, for simplicity assuming constant Δx, the parameter value A contributes to this grid point and its neighbors as

$$\begin{pmatrix} \delta A_{j+1} \\ \delta A_j \\ \delta A_{j-1} \end{pmatrix}^{n+1} = A_j^n \begin{pmatrix} 0 \\ 1 \\ 0 \end{pmatrix} + A_j^n s \begin{pmatrix} 1 \\ -2 \\ 1 \end{pmatrix}, \tag{11}$$

where the first term on the right represents the unchanged state, and the second term represent the discrete increment of the 'source term' for smoothing. Using the source term expression for the DIA of Eq. (6), considering that it is applied for component 1 of the quadruplet coinciding with each discrete spectral grid point individually, the effects of the interactions according to the DIA can be written in a distribution form similar to Eq. (11) as

$$\begin{pmatrix} \delta F_3 \\ \delta F_1 \\ \delta F_4 \end{pmatrix}^{n+1} = F_1^n \begin{pmatrix} 0 \\ 1 \\ 0 \end{pmatrix} + F_1^n \frac{S\Delta t}{F_1^n} \begin{pmatrix} 1 \\ -2 \\ 1 \end{pmatrix}, \tag{12}$$

with S representing the scalar strength of the interactions in Eq. (6)

$$S = Cg^{-4}f_1^{11}\left[F_1^2\left(\frac{F_3}{(1+\lambda)^4} + \frac{F_4}{(1-\lambda)^4}\right) - \frac{2F_1F_3F_4}{(1-\lambda^2)^4}\right], \tag{13}$$

evaluated at the beginning of the discrete time step (n). Clearly, the nature of the interactions according to the DIA is similar to that of a traditional diffusion operator, with the exception that the diffusion

Eq. (11) operates on neighboring discrete grids points, whereas the DIA Eq. (12) operates along a locus of interactions on wave components in a quadruplet.

The similarity and differences are illustrated further in Fig. 1 with typical DIA quadruplet layouts for a typical spectral grid with $X_f = 1.1$ and $\Delta\theta = 15°$. Fig. 1a shows a typical model configuration where the DIA quadruplet samples spectral space over scales larger that the discretization of the spectral space. In other words, this quadruplet is resolved by the spectral discretization. Since the quadruplet generally does not consider adjacent discrete spectral grid points, the results of this scheme are not expected to closely resemble the characteristics of a diffusion equation.

Fig. 1b shows a quadruplet with $\lambda = 0.03$, which samples spectral space over much smaller scales. This quadruplet entirely falls within a nine grid point stencil around a central grid point coinciding with component 1 of the quadruplet. Hence the spectral grid does not resolve the quadruplet, and Eq. (12), with the appropriate redistribution of interaction contributions to adjacent discrete grid points (as will be discussed below), considers neighboring spectral grid points only. Thus, for unresolved quadruplets with small λ, the DIA approach indeed closely resembles a diffusion operator. Moreover, for small time steps Eq. (12) remains a conventional source term. As will be shown below, this source term operates locally, and it can remain small compared to the DIA in a traditional configuration. Hence, its impact on overall model results is local in the spectrum. For large time steps, stability will typically require that $S\Delta t/F$ is limited, consistent with the stability criterion of the diffusion equation. Using such a limitation, the source term naturally morphs into a filter with well defined stability criteria.

A diffusion-like filter approach based on the DIA differs from previously suggested diffusion approaches of Zakharov and Pushkarev (1999) and Jenkins and Phillips (2001) in several ways. The latter approaches enforce the conservative behavior of the nonlinear interactions by choosing an appropriate higher order diffusion formulation. In Eqs. (12) and (13) the conservative properties are enforced by applying the changes along the locus of interactions rather than the discrete grid lines. Applying the changes in this way is a sufficient requirement for conservation of action, energy and momentum, both in continuous (Webb, 1978), and discrete spaces (Tolman, 2008, Section 2.2). This results in an approach that is equivalent, but not fully equal to a lowest order diffusion approach.

Considering the similarity between the unresolved DIA and a simple diffusion approach as illustrated above, and considering the close links between diffusion, smoothing and filtering, a DIA-based filter for the WAVEWATCH III^{reg} model (Tolman et al., 2002; Tolman, 2009b, henceforth denoted as WW3) is developed here. The filter is applied after source term integration has been performed, and hence does not represent an additional source term, nor does it interface with the source term integration directly. The development of the filter requires several steps.

(i) Conversion of the traditional DIA source term to spectral definitions used in WW3. Note that the traditional DIA implementation in WW3 is expressed in terms of the energy density spectrum $F(f,\theta)$, using Jacobian transformations to convert spectra and source terms. Here, a more elegant expression directly in terms of the internal spectral description of WW3 is used.

(ii) Applying the DIA to the discrete spectral grid rather than an interaction locus, while accounting for multiple quadruplet realizations for a single quadruplet definition.

(iii) Localization of the DIA in spectral space so that it applies only to frequencies in the equilibrium range of the spectrum.

(iv) Limitation of the source term strengths so that the source term naturally transitions into a strong but stable filter (smoother).
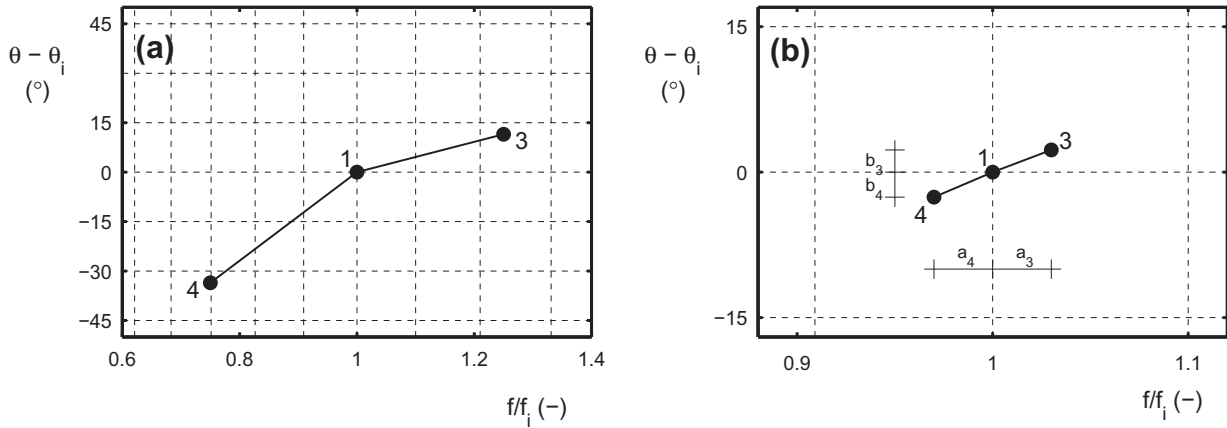
Fig. 1. Layout of quadruplets of the DIA according to Eq. (2) through (5) on a spectral grid with $X_f = 1.1$ and $\Delta\theta = 15°$. (a) Typical layout for DIA in operational models with $\lambda = 0.25$. (b) Unresolved quadruplet with $\lambda = 0.03$. (f_i, θ_i) is the discrete grid point aligned with quadruplet component 1. Dashed lines represent discrete grid lines. $a_{3,4}$ and $b_{3,4}$ represent relative quadruplet offsets (fractions of distances between discrete grid lines) in corresponding boxes spanned by grid points.

The WW3 model is based on an action balance equation (Bretherthon and Garrett, 1968) to account for wave current interactions, and describes the spectral phase space in terms of wavenumber k and direction θ. The corresponding action density spectrum $N(k,\theta)$ is related to the energy density spectrum $F(f,\theta)$ as

$$N(k,\theta) = \frac{c_g}{2\pi} \frac{F(f,\theta)}{\sigma}, \tag{14}$$

where c_g is the group velocity $c_g \equiv \partial\sigma/\partial k$. For this spectrum, a balance equation similar to Eq. (1) is solved, and the DIA equation for individual discrete interaction contributions equivalent to Eq. (6) is given as Tolman (2008, Section 2.7)

$$\begin{pmatrix} \delta S_{nl,1} \\ \delta S_{nl,3} \\ \delta S_{nl,4} \end{pmatrix} = \begin{pmatrix} -2 \\ 1 \\ 1 \end{pmatrix} \frac{Ck^4\sigma^{12}}{(2\pi)^9 g^4 c_g} \left[\frac{N_1^2}{k_1^2}\left(\frac{N_3}{k_3} + \frac{N_4}{k_4}\right) - 2\frac{N_1}{k_1}\frac{N_3}{k_3}\frac{N_4}{k_4} \right], \tag{15}$$

where the scaling function is developed so that C is equal to C in Eq. (6). The corresponding version of Eqs. (12) and (13) are given as

$$\begin{pmatrix} \delta N_3 \\ \delta N_1 \\ \delta N_4 \end{pmatrix}^{n+1} = N_1^n \begin{pmatrix} 0 \\ 1 \\ 0 \end{pmatrix} + N_1^n \frac{S\Delta t}{N_1^n} \begin{pmatrix} 1 \\ -2 \\ 1 \end{pmatrix} \tag{16}$$

and

$$S = \frac{Ck^4\sigma^{12}}{(2\pi)^9 g^4 c_g} \left[\frac{N_1^2}{k_1^2}\left(\frac{N_3}{k_3} + \frac{N_4}{k_4}\right) - 2\frac{N_1}{k_1}\frac{N_3}{k_3}\frac{N_4}{k_4} \right]. \tag{17}$$

The next step is to convert the changes along interaction loci in Eq. (16) to changes in the discrete spectral grid. This requires redistribution over discrete grid points consistent with linear interpolation, using relative distances a_3 through b_4 in Fig. 1b. Furthermore, the resonance conditions for the DIA from Eq. (2) through (5) result in two mirror image quadruplets, which can be obtained by changing the signs of the directional offsets of quadruplet components 3 and 4. To ensure symmetry in the resulting interactions, both quadruplet realizations need to be accounted for. In the discrete spectral grid, the equivalent redistribution algorithm then becomes

$$M_\delta^{n+1} = N_{i,j}^n M_c + N_{i,j}^n \left[\frac{M_c S_a \Delta t}{N_{i,j}^n} M_a + \frac{M_c S_b \Delta t}{N_{i,j}^n} M_b \right], \tag{18}$$

with

$$M_\delta = \begin{pmatrix} \delta N_{i-1,j+1} & \delta N_{i,j+1} & \delta N_{i+1,j+1} \\ \delta N_{i-1,j} & \delta N_{i,j} & \delta N_{i+1,j} \\ \delta N_{i-1,j-1} & \delta N_{i,j-1} & \delta N_{i+1,j-1} \end{pmatrix}, \quad M_c = \begin{pmatrix} 0 & 0 & 0 \\ 0 & 1 & 0 \\ 0 & 0 & 0 \end{pmatrix}, \tag{19}$$

$$M_a = \begin{pmatrix} a_4 b_4/M_c & (1-a_4)b_4/M_c & 0 \\ a_4(1-b_4)/M_c & -1 & a_3(1-b_3)/M_c \\ 0 & (1-a_3)b_3/M_c & a_3 b_3/M_c \end{pmatrix}, \tag{20}$$

$$M_b = \begin{pmatrix} 0 & (1-a_3)b_3/M_c & a_3 b_3/M_c \\ a_4(1-b_4)/M_c & -1 & a_3(1-b_3)/M_c \\ a_4 b_4/M_c & (1-a_4)b_4/M_c & 0 \end{pmatrix}, \tag{21}$$

$$M_c = -(a_3 b_3 + a_4 b_4 - a_3 - a_4 - b_3 - b_4), \tag{22}$$

where $N_{i,j} = N(k_i, \theta_j)$, a_3, a_4, b_3 and b_4 are defined as in Fig. 1b, and S_a represent the interaction strength of Eq. (17) for the quadruplet realization with a positive offset angle for quadruplet component 4 and a negative offset angle for quadruplet component 3, and S_b represents the corresponding strength for the quadruplet realization with opposite signs of offset angles.

Assuming for simplicity that $S_a \approx S_b$, the smoothing stencil of the DIA becomes $M_a + M_b$. Furthermore assuming that $a_3 \approx a_4 \approx b_3 \approx b_4$ the layout of this stencil is easily addressed for various levels of resolution of the quadruplet by the grid. With these assumptions, a borderline resolved quadruplet with $a_3 = 1$, a poorer resolution with $a_3 = 1/3$, and a severely unresolved quadruplet with $a_3 \ll 1$ result in a stencil $M_a + M_b$ of

$$\begin{pmatrix} 0.5 & 0 & 0.5 \\ 0 & -2.0 & 0 \\ 0.5 & 0 & 0.5 \end{pmatrix}, \quad \begin{pmatrix} 0.1 & 0.4 & 0.1 \\ 0.4 & -2.0 & 0.4 \\ 0.1 & 0.4 & 0.1 \end{pmatrix}$$

and

$$\begin{pmatrix} 0 & 0.5 & 0 \\ 0.5 & -2.0 & 0.5 \\ 0 & 0.5 & 0 \end{pmatrix},$$

respectively. The stencil for the almost resolved case ($a_3 = 1$) indicates that the diffusion occurs diagonally in the discrete grid. When the quadruplet is severely unresolved ($a_3 \ll 1$), the diffusion lines up with the grid axes. In between, the diffusion has a clear two-dimensional nature.

So far, the nonlinear formulation of Eq. (16) through (22) are simply a reformulation of the full DIA interactions of Eq. (15), but are otherwise identical. To convert it to a high-frequency filter,

the expressions need to be localized in spectral (frequency) space. A simple way to achieve this without compromising the overall conservative properties of the parameterization is to filter individual interaction strengths S_a and S_b for given quadruplets. A simple high-pass filter is adopted here, taken from the JONSWAP study (Hasselmann et al., 1973)

$$\Phi(f) = \exp\left[-c_1\left(\frac{f}{c_2 f_p}\right)^{-c_3}\right], \tag{23}$$

where c_1 through c_3 are tunable parameters. The latter three parameters need to be chosen such that $\Phi(f_p) \approx 0$, $\Phi(f > 3f_p) \approx 1$ and that $\Phi \approx 0.5$ for frequencies moderately larger than f_p. This can be achieved by setting

$$c_1 = 1.25, \quad c_2 = 1.50, \quad c_3 = 6.00. \tag{24}$$

Note that the filter $\Phi(f)$ and the process it describes will henceforth be identified as localization rather than filtering, to avoid confusing frequency filtering with spectral filtering. Adding the frequency localization, the nondimensional discrete changes per quadruplet at the central grid point of the stencil $\widetilde{S}_a$ and $\widetilde{S}_b$ are defined as

$$\widetilde{S}_a = \Phi(f)M_c S_a \Delta t / N_{i,j}^n, \quad \widetilde{S}_b = \Phi(f)M_c S_b \Delta t / N_{i,j}^n, \tag{25}$$

and Eq. (18) can be written as

$$\boldsymbol{M}_\delta^{n+1} = N_{i,j}^n \boldsymbol{M}_c + N_{i,j}^n\left[\widetilde{S}_a \boldsymbol{M}_a + \widetilde{S}_b \boldsymbol{M}_b\right], \tag{26}$$

which effectively becomes a two-dimensional version of the general diffusion Eq. (11).

Finally, the localized source term (26) needs to be converted into a filter for interaction strengths and/or time steps which would otherwise result in unstable model integration. The diffusion Eq. (9) or (11) can be converted into a constant strength filter by setting the discretization parameter s of Eq. (9) to a pre-set value satisfying Eq. (10). By dynamically and locally limiting s to satisfy Eq. (10) while using the redistribution form of the diffusion equation of Eq. (11), both conservation properties and stability of the numerical approach are retained and the diffusion operator naturally morphs into a filter when needed. Similarly, the source term (26) can naturally become a filter by limiting $\widetilde{S}_a$ and $\widetilde{S}_b$ to a preset maximum value. Defining a general maximum value $\widetilde{S}_{max}$, the maximum values per quadruplet realization $\widetilde{S}_{m.a}$ and $\widetilde{S}_{m.b}$ are defined as

$$\widetilde{S}_{m,a} = \frac{|\widetilde{S}_a|\widetilde{S}_{max}}{|\widetilde{S}_a| + |\widetilde{S}_b|}, \quad \widetilde{S}_{m,b} = \frac{|\widetilde{S}_b|\widetilde{S}_{max}}{|\widetilde{S}_a| + |\widetilde{S}_b|}, \tag{27}$$

after which the normalized changes $\widetilde{S}_a$ and $\widetilde{S}_b$ are limited to satisfy the following inequalities

$$-\widetilde{S}_{m,a} \leqslant \widetilde{S}_a \leqslant \widetilde{S}_{m,a}, \quad -\widetilde{S}_{m,b} \leqslant \widetilde{S}_b \leqslant \widetilde{S}_{m,b}. \tag{28}$$

Based on a comparison with the diffusion equation, values of $S_{max} \approx 0.5$ are expected to result in a stable filter.

Note that limitation of Eq. (28) is rather crude and discontinuous in its derivatives. Experiments with a smoother transition based on hyperbolic tangent functions proved to have little if any impact on model results, but required significantly more computational time, making Eq. (28) preferable. Similarly, the distribution of maxima according to Eq. (27) is somewhat subjective, but proved adequate in numerical experiments.

4. Parameter settings

Optimal parameter settings and filter behavior are assessed in three steps. First, the effect of the quadruplet layout on the shape of the interactions in spectral space is assessed. With a chosen quadruplet layout, the strength of the interactions then is varied

without invoking the limiter to find an appropriate strength C of the filter. Finally, the effect of the limitation of the changes per quadruplet is tested to obtain practical values for $\widetilde{S}_{max}$ required for stable filter behavior.

The essence of the filter is that the quadruplet is not resolved by the discrete spectral grid. Therefore, the filter should be defined by the resolution of the quadruplet rather than the quadruplet parameter λ. This is achieved by introducing a relative resolution a_{34} (representing $a_{3,4}$), from which λ is computed as

$$\lambda = a_{34}(X_f - 1), \tag{29}$$

implicitly assuming that the directional and frequency resolutions are similar.

To investigate the shape in spectral space of the interaction on which the filter is based, a test spectrum was obtained from the WW3 wave model. The spectrum was generated using the interactive test as provided with the model code.[1] The spectrum and nonlinear interactions according to the default DIA are presented in Fig. 2a and b. Panels c through f show the DIA with the frequency localization Φ of Eqs. (23) and (24) added, and with a_{34} set to 1.00, 0.33, 0.10 and 0.05, respectively. The strength C is selected for convenience of plotting only so that the magnitude of the localized DIAs is similar to that of the full DIA at higher frequencies. Note that these results were obtained from the test spectrum, but that the new filter was not included in the model integration from which the test spectrum was obtained. Note, furthermore, that the requirement to dramatically increase C with decreasing λ (or a_{34}) to obtain interactions of similar strength is consistent with previous results of, for instance, Tolman and Krasnopolsky (2004).

For all versions of the localized DIA (Fig. 2c through f) Φ ensures that interactions occur only at frequencies above the spectral peak frequency, unlike for the full DIA (Fig. 2b). For $a_{34} = 1.00$ (Fig. 2c) interactions occur at relatively large scales in spectral space. For decreasing a_{34} (Fig. 2d–f) interactions occur at smaller scales, and for $a_{34} < 0.10$ (Fig. 2e and f) the shape of the localized interactions effectively becomes independent of a_{34}. This suggest that for $a_{34} < 0.10$ the choice of a_{34} becomes irrelevant, as long as C is chosen consistently with a_{34}. Considering this, $a_{34} = 0.05$ is used as the default value in WW3.

With the frequency localization defined by Eq. (24) and $a_{34} = 0.05$, the localized DIA is added to the default wave model. With $\widetilde{S}_{max} = 10^5$ any limitation is removed from the filter, and the impact of an increasing strength C on model stability can be investigated. For an interaction strength $C = 10^9$ the first minor impact on the model integration is observed. For $C = 10^{10}$ the added source term is impacting and destabilizing the model integration (figures not presented here). Note that the underlying wave model is fully stable, and that the instability is introduced here solely by the new filter without the appropriate limitation $\widetilde{S}_{max}$. This makes a filter with $a_{34} = 0.05$ and $C = 10^{10}$ a good starting point to assess the potential of using the limiter $\widetilde{S}_{max}$ to stabilize the model integration. Fig. 3 shows model results corresponding to Fig. 2 obtained by integrating the model with the new filter added with $\widetilde{S}_{max} = 2.00$, 1.00, 0.50 and 0.25, respectively. The resulting full DIA source terms are shown instead of the spectrum, since these source terms proved more sensitive to adding the filter than the spectrum.

Based on a comparison with a simple diffusion equation, it is expected that $\widetilde{S}_{max} \approx 0.5$ will result in stable model integration with the filter included. Note that the transition from stable to unstable model integration is not expected to be sharp here, as the DIA in WW3 is expected to counterbalance initial unstable

---

[1] Using the spectrum for the output point identified as "Point 4" after 4 h of model integration, $X_f = 1.1$, $\Delta\theta = 15°$.
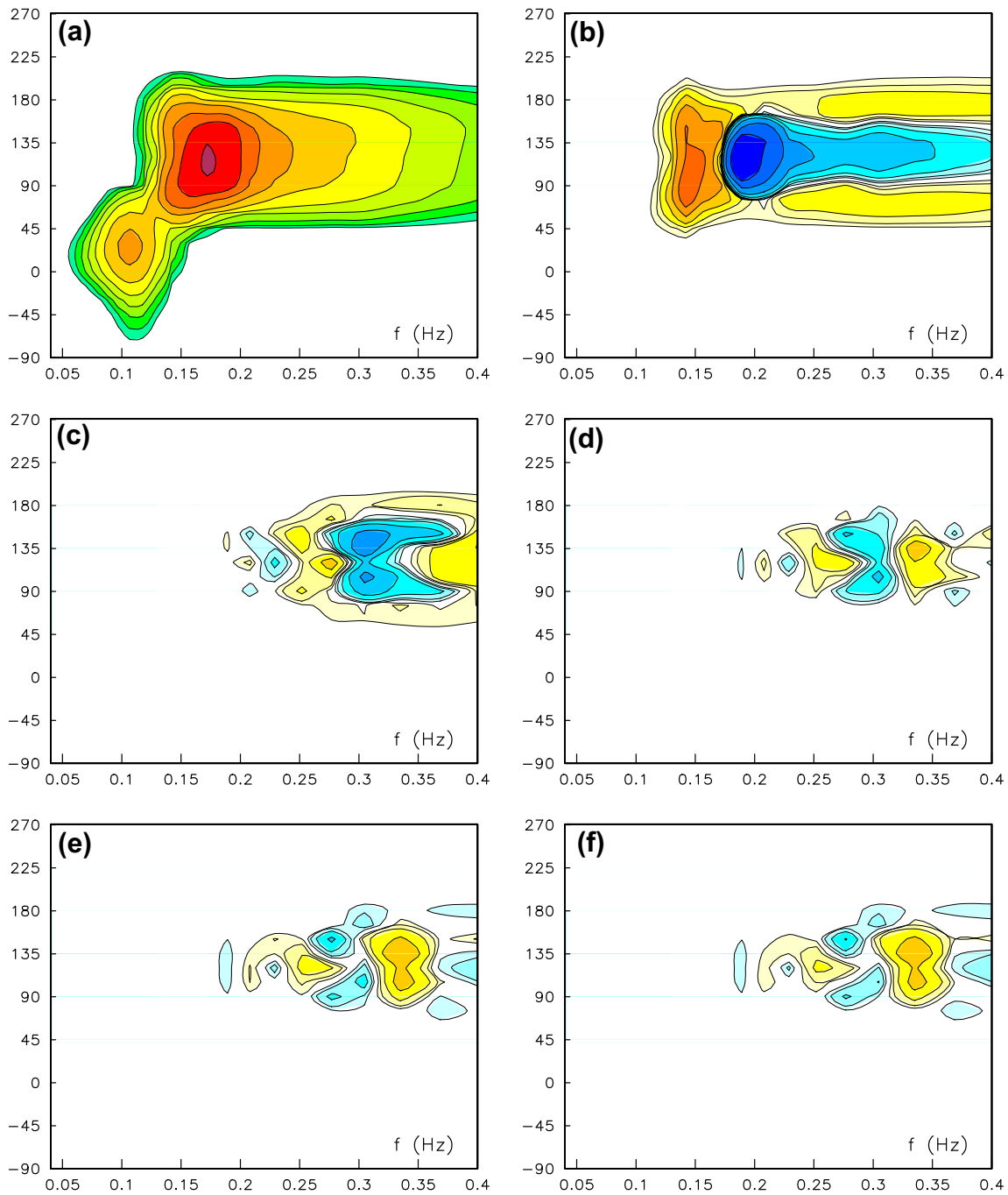
Fig. 2. (a) Test spectrum $F(f, \theta)$ and (b) corresponding nonlinear interaction $S_{nl}(f, \theta)$ according to the DIA. (c–f) Localized source term without limitation on interaction strength. (c) $a_{34} = 1.00$, $C = 2 \times 10^8$. (d) $a_{34} = 0.33$, $C = 4 \times 10^9$. (e) $a_{34} = 0.10$, $C = 4 \times 10^{10}$. (f) $a_{34} = 0.05$, $C = 7 \times 10^{10}$. Logarithmic scaling with contours at factor 2 increments and lowest contours at 2×10^{-2} m^2 s for spectrum and $\pm 1 \times 10^{-5}$ m^2 for the source terms; blues correspond to negative values in source term plots.

behavior of the filter. As expected, values of $\widetilde{S}_{max}$ significantly larger than 0.5 ($\widetilde{S}_{max} = 2$, Fig. 2a) result in unstable model integration, whereas $\widetilde{S}_{max} \approx 0.5$ (Fig. 2b-d) indeed results in stable model integration. For $\widetilde{S}_{max} = 0.25$ (Fig. 2d), the filter has no notable impact on model integration. Note that $\widetilde{S}_{max} = 0.25$ allows for the filter to be strong, with the underlying source term displaying time scales of change equivalent to the numerical time step Δt. Simultaneously, however, stable model integration with a spectral shape close to an equilibrium shape will naturally reduce the strength of the filter dramatically, explaining a small or negligible impact for a potentially strong filter.

Considering the above results, the default filter settings in WAVEWATCH III are defined by (24), $a_{34} = 0.05$, $C = 10^{10}$, and

$\widetilde{S}_{max} = 0.25$. In the model setup, all these parameters can easily be redefined by the user through namelists in input files (as for other source term parameters in Tolman, 2009b).

5. Applications

So far, the testing of the filter has only focused on the stability of the filter, and on the filter not adversely influencing model integration in the otherwise default settings of the WW3 wave model. In the latter model, the filter adds approximately 10% to the computational time, whereas decades of experience with a traditionally configured DIA have shown that additional filtering is
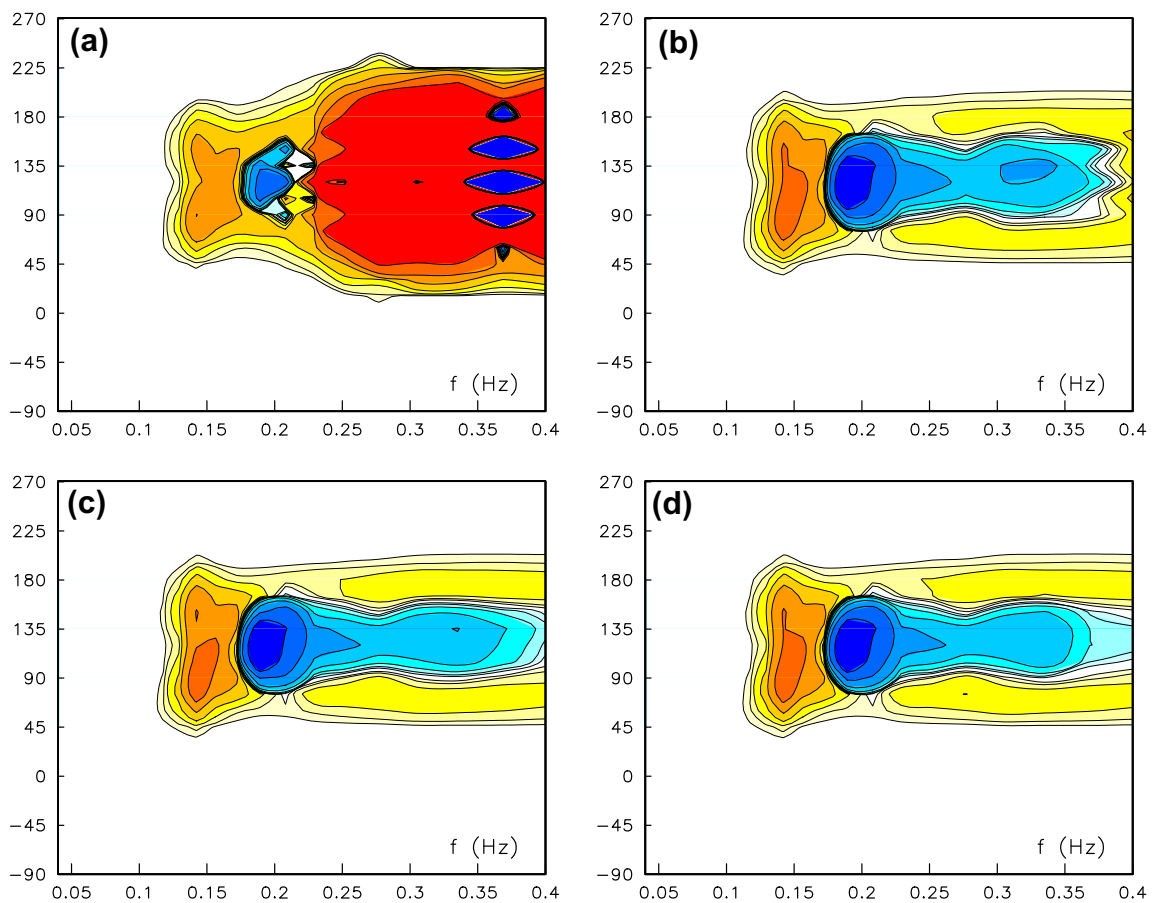
Fig. 3. Source term obtained by model integration with the filter added with $a_{34} = 0.05$, $C = 10^{10}$ and (a) $\widetilde{S}_{max} = 2.00$, (b) $\widetilde{S}_{max} = 1.00$, (c) $\widetilde{S}_{max} = 0.50$, (d) $\widetilde{S}_{max} = 0.25$. Spectrum and legend as in Fig. 2.

not needed in such a model configuration. As mentioned in the introduction, the filter was designed for models using interaction approximations with inherent noise issues at high frequencies. Two such model configurations will be addressed here. The first is a WW3 model using a Neural Network interaction approximation as reported in Tolman (2009a). The second is a WW3 configuration using a Generalized Multiple DIA (GMD) configuration as reported in Tolman (2010).

Attempts to produce a Neural Network Interaction Approximation (NNIA) have been reported in Tolman and Krasnopolsky (2004), Tolman et al. (2005), Tolman (2009a) and Wahle et al. (2009). In Tolman (2009a) it is shown that a successful NNIA needs to incorporate at least four elements.

(i) A Neural Network (NN) approach to estimate the interactions from the spectrum.
(ii) An explicit estimate of the error (ϵ) of the NN obtained by estimating the spectrum from the source term with an 'inverse' NN (e.g., Krasnopolsky and Schiller, 2003; Krasnopolsky et al., 2008).
(iii) A fall-back interaction approximation to be used when the error estimate ϵ indicates that the NN is insufficiently accurate.
(iv) An explicit way to deal with build-up of noise in the spectrum at spectral scales that are not resolved by the NN.

In Tolman (2009a) an NNIA is developed to reproduce the exact interactions, and is tested in numerical model integration in WW3, and the exact interactions are used as the corresponding fall-back

approximation. In Fig. 4 the evolution of the NN error ϵ is presented for various model configurations.

The solid green line in Fig. 4 represents the NN error obtained by integrating the model with the exact interactions, and using the NNIA only to estimate the error ϵ. Large values on this error
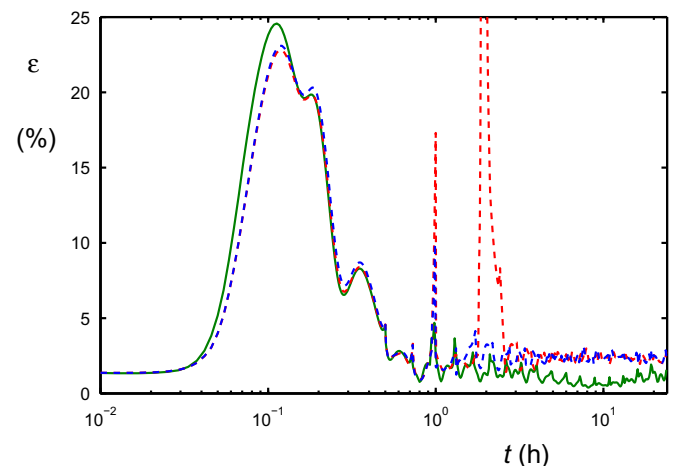

Fig. 4. Evolution in time t of the NN error ϵ for a wave growth test. Green line: model integration based on exact interactions. Dashed red line: Model integration based on NNIA without filter, Dashed blue line. Model integration based on NNIA with filter. (from Tolman, 2009a). (For interpretation of the references to colour in this figure legend, the reader is referred to the web version of this article.)

in the early stages of the integration ($t < 1$ h) indicate that the NN is not sufficiently trained to provide accurate interactions in these conditions. Small errors for the green line for $t > 1$ h indicate that the NNIA is accurate enough to be used in model integration.

The dashed lines in Fig. 4 represent results obtained with model integration using the NNIA for $\epsilon \leqslant 2.5\%$, where the red line is obtained without using the filter, and the blue line is obtained with the filter. Without the filter (red line), spikes in errors ϵ are observed for $t \approx 1$ h and $t \approx 2$ h. The first spike is partially removed by the filter, and the second spike is completely removed by the filter (compare red and blue lines). Close inspection of associated spectra shows that the error spikes are associated with spurious behavior (noise) in the high-frequency part of the spectrum at small scales in spectral space (figures not presented here). The associate growth in NN error ϵ indicates that this noise is not resolved by the NN. The new filter appears to be able to remove this noise and the associated large errors ϵ. Furthermore, the filter reduces the need for using the fall-back exact interaction computations, effectively speeding up the model integration by 27%. This specific case is representative for many such wave growth experiments using a NNIA, and typically a model speed-up of 20 to 30% is found. Whereas the filter does not appear capable of fully removing small-scale noise from the model (see Tolman, 2009a, for a more detailed discussion), it clearly contributes positively to the overall model behavior when using the NNIA in a full wave model.

The second nonlinear interaction approximation with which the new filter is used is the GMD developed by Tolman (2009a, 2010). This interaction approximation expands upon the DIA by:

(i) Expanding the definition of the representative quadruplet to effectively arbitrary configurations by augmenting the one-parameter quadruplet definition of Eq. (5) with two- and three-parameter definitions.
(ii) Using multiple representative quadruplets.
(iii) Expanding the DIA from a deep water formulation to a formulation for arbitrary water depths.

In the above studies, the free parameters in many GMD configurations are objectively optimized to represent full model integration results as obtained with the exact interactions for a set of idealized test cases.

Expanding the definition of a representative quadruplet in the GMD may lead to GMD configurations that are not computationally stable (e.g., Tolman, 2003; Tolman and Krasnopolsky, 2004). The objective optimization of GMD configurations in Tolman (2009a), Tolman (2010), however, naturally selects stable configurations. In a small subset of objectively optimized near-optimum GMD configurations the objective optimization does allow for spurious high-frequency noise in a small subset of spectra and a small subset of test cases. This is illustrated in Fig. 5 with near-shore model results for a slanting fetch case and a GMD configuration with five quadruplets using a two-parameter quadruplet definition (see Tolman, 2010 for more details of this configuration). The slanting fetch case considers wave growth offshore from a straight coastline, with offshore winds under a 45° angle with the coast. Adding the new filter to the model while leaving the GMD unchanged effectively removes all high-frequency noise from the spectrum. This is illustrated in Fig. 6. Moreover, objective error measures
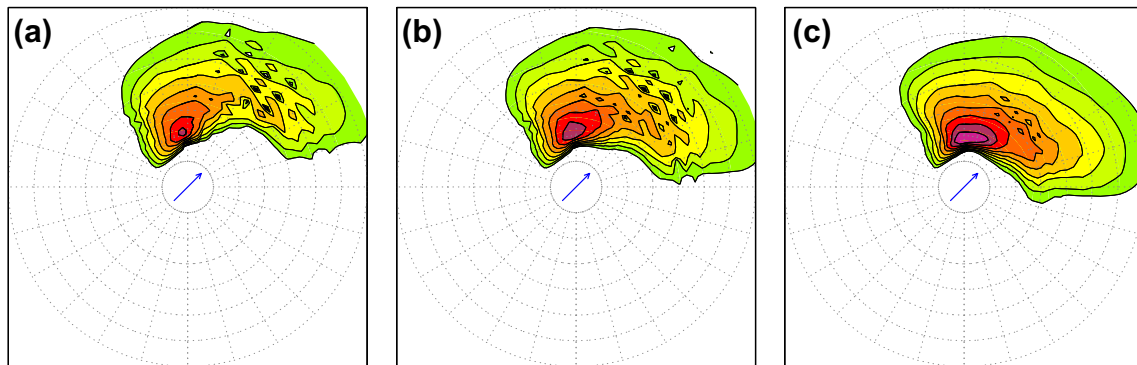

Fig. 5. Spectra from a slanting fetch test case with 10 km resolution at (a) 10, (b) 30, and (c) 100 km offshore. Arrow identifies wind direction, offshore direction to the west. Computations with GMD with 5 quadruplets with two-parameter quadruplet definition (see Tolman, 2010). $X_f = 1.07$, $\Delta\theta = 10°$.
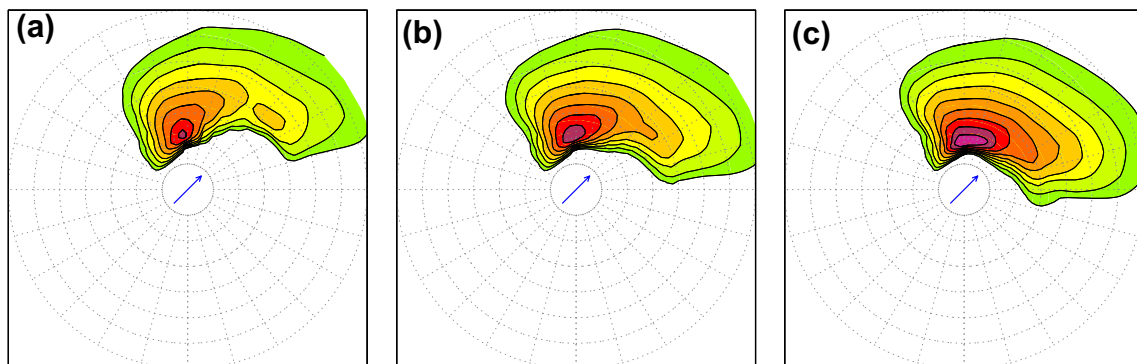

Fig. 6. Like Fig. 5 with filter added.

used in optimizing the GMD show that the model with filter more closely represents the model based on the exact interactions, even though the filter was not used in the model optimization. This strongly indicates that the filter is able to remove high-frequency noise from the model with minor impact on overall model behavior. In this case, the filter did not significantly impact the model integration time, implying that the additional computational effort used by the filter was offset by a slightly smoother and faster integration.

6. Discussion and conclusions

The present study addresses filtering of the high-frequency range of wind wave spectra. Such a filter can be used to augment nonlinear interaction approximations, and can potentially speed up model integration using dynamic time stepping. In the latter case, the filter is expected to remove noise with small evolutionary time scales and ensure that the model remains close to a spectral equilibrium in this range of the spectrum. For both applications, it is essential that the filter incorporates the conservation properties of the nonlinear interactions, and by extension, is consistent with stationary solutions of the interactions. It should be noted that such a filter is not a prerequisite of third generation wave models, but may be useful in combination with selected parameterizations of nonlinear interactions as demonstrated in this study.

Starting with the traditional Discrete Interaction Approximation (DIA, Hasselmann et al., 1985), and applying this to resonant interactions on spectral scales that are not resolved by the discrete spectral grid, a numerical source term formulation is found that closely resembles a traditional lowest-order diffusion equation. Localizing the interaction strengths in frequency space allows for application at high frequencies only, while retaining all conservation properties (and asymptotic solutions) of the nonlinear interactions. Limiting the local changes in the spectrum consistent with stability criteria for the numerical implementation of diffusion equations naturally morphs this source term into a filter for conditions where the source term time scales are smaller than numerical time steps in the wave model. Note that this degenerated (non-resolved) DIA results in a *conservative* quasi-diffusion approach due to the resonance conditions being satisfied for each quadruplet (Webb, 1978). Without using this property of nonlinear interactions, only higher-order conservative diffusion approaches can be found as in Zakharov and Pushkarev (1999), Jenkins and Phillips (2001).

Free parameters in this filter (source term) have been estimated using traditional wave growth conditions in the WAVEWATCH III (WW3) wave model. If the free quadruplet parameter λ is chosen small enough that relative offsets a_{34} in the quadruplet are less than 10% of the discrete spectral grid size, the shape in spectral space of the interactions effectively becomes independent of λ. Setting the relative offsets to 5% requires the interaction strength to be $C = 10^{10}$ to become strong enough to influence model integration results. When normalized interactions strengths then are limited to $\widetilde{S}_{max} \approx 0.25$, the filter is numerically stable as expected, potentially allowing for strong numerical smoothing associated with expected maximum values of $\widetilde{S}_{max}$, yet not influencing model integration in the smooth and stable integration of the default WW3 model settings. Because the underlying wave model configuration does not require a filter to suppress high frequency noise, the non-impact of this filter with these established parameter settings should be considered a strength of the approach.

It should be noted that by definition, (some of) the settings of the filter will be sensitive to the discretization of the spectral space. The frequency localization and limiter $\widetilde{S}_{max}$ are not associated with the spectral resolution. The directional resolution $\Delta\theta$ is only indirectly associated with the filter behavior. As long as $b_{3,4} \ll 1$, the resolution is not expected to have a notable impact on results. This implies that the filter settings only need to be re-addressed for models with high directional and low frequency resolution. The frequency resolution X_f does have a direct impact on the filter behavior. With changing X_f, λ will change for a given a_{34} according to Eq. (29). Considering that the shape of the interactions was shown to be insensitive to a_{34} and hence λ for sufficiently small a_{34}, this is not expected to have a direct impact on the shape of the interactions. However, optimum values C for a DIA are known to increase with decreasing λ (as discussed above), and hence the optimum value of C of the filter is expected to become a function of λ, and it is prudent to reassess this value if spectral resolutions are changed.

Whereas optimum values of C should be dependent on the spectral resolution, such a dependency is not expected to be extreme. This is illustrated here with the experience that the model parameters were estimated with a conventional operational spectral resolution ($X_f = 1.10, \Delta\theta = 15°$), after which they were successfully applied to models with a more research-oriented spectral resolution ($X_f = 1.07, \Delta\theta = 10°$) without retuning.

Considering this dependency, two refinements to the filter could be considered. First, a functional dependency of C on ($X_f, \Delta\theta$) could be established to make the filter and its parameter settings more universal. Second, it might be possible to estimate C on more theoretical ground, by attempting to mimic restoration time scales of spectral disturbances from exact interactions with experiments as introduced by Young and Van Vledder (1993). Considering the pragmatic nature of the present filter, such refinements have not been considered here, but could be considered for future research.

After having established parameter settings for the filter, it has been applied to model configurations known to incorporate high-frequency spectral noise. Model configurations considered include a Neural Network Interaction Approximation (NNIA) and a Generalized Multiple DIA (GMD). In the former case the filter is shown to suppress error growth in the NNIA as well as speed up computations significantly. In the latter case, the filter is shown to remove spurious high-frequency noise, and results in more accurate model behavior. Note that in both cases the filter was applied after the corresponding interaction approximations were optimized. Tentatively, both approaches might benefit from including the filter during the development of the parameterization. A first step would be to include the filter while performing the optimization experiments. Furthermore, optimization of parameter setting of the filter could be explicitly performed during the development of the parameterization. Particularly the genetic optimization techniques used to optimize the GMD (e.g., Tolman and Krasnopolsky, 2004; Tolman, 2009a) are naturally suited to objectively optimize free parameters in the new filter formulation.

It should be noted that the limiter is consistent with an f^{-4} spectral shape, as this spectral shape is an equilibrium solution where the term in square brackets in Eqs. (6) and (15) vanishes. In WW3, a parametric tail with an f^{-5} shape is applied for frequencies $f > 3f_p$, consistent with the transition in spectral shape observed in nature (e.g., Long and Resio, 2007). If the above parametric tail is not used for $f > 3f_p$, but instead the model is allowed to dynamically find a source term equilibrium for higher frequencies, it may become necessary to further localize the filter in frequency space by also suppressing it for frequencies substantially larger than $3f_p$.

In this context it is also prudent to recognize that the equilibrium solution implicit to the filter is associated with the equilibrium solution of the DIA and its highly limited interaction configuration. It is bound to deviate from the detailed spectral shapes imposed by the full interactions, as the interaction configurations used by the DIA do not represent dominant configurations away from the spectral peak (e.g., Webb, 1978). The filter should

therefore not be seen as the main mechanism to impose spectral shapes, unless objective optimization techniques mentioned above prove it adequate.

The filter includes a limiter on the maximum change allowed per interacting quadruplet [Eqs. (27) and (28)]. This limiter is non-local, as it operates on nine spectral grid points simultaneously, and is fully conservative with respect to action, energy and momentum. This is in contrast with limiters used to stabilize source term integration (e.g., Hersbach and Janssen, 1999; Hersbach and Janssen, 2001; Hargreaves and Annan, 1998; Hargreaves and Annan, 2001; Tolman, 2002), which are local in spectral space and non-conservative. The latter limiters are needed mostly to suppress spurious waves in the spectral shape. It may be possible to use the new nonlinear filter and its conservative limitation as a blueprint to develop conservative limiters to stabilize source term integration, particularly when mean and oscillating integration solutions are separated as in the asymmetric limiter suggested by Tolman (2002). However, since the WW3 model does not rely on limiters to stabilize source term integration, this has not been explored further here.

The new filter is intended to be included as an option in the next public release of WAVEWATCH III, and is presently available to co-developers of this model through the NCEP subversion server.

Acknowledgments

References

Bretherthon, F.P., Garrett, C.J.R., 1968. Wave trains in inhomogeneous moving media. Proc. Roy. Soc. London A 302, 529–554.

Fletcher, C.A.J., 1988. Computational Techniques for Fluid Dynamics, Part I and II. Springer, pp. 409–484.

Hargreaves, J.C., Annan, J.D., 1998. Integration of source terms in WAM. In: Proceedings of the Fifth International Workshop on Wave Forecasting and Hindcasting, pp. 128–133.

Hargreaves, J.C., Annan, J.D., 2001. Comments on "improvement of the short fetch behavior in the ocean wave model (WAM)". J. Atmos. Oceanic Tech. 18, 711–715.

Hasselmann, K., 1960. Grundgleichungen der seegangsvoraussage. Schiffstechnik 7, 191–195.

Hasselmann, K., 1962. On the non-linear energy transfer in a gravity wave spectrum, part 1. General theory. J. Fluid Mech. 12, 481–500.

Hasselmann, K., 1963. On the non-linear transfer in a gravity wave spectrum, part 2, Conservation theory, wave-particle correspondence, irreversibility. J. Fluid Mech. 15, 273–281.

Hasselmann, K., Barnett, T.P., Bouws, E., Carlson, H., Cartwright, D.E., Enke, K., Ewing, J.A., Gienapp, H., Hasselmann, D.E., Kruseman, P., Meerburg, A., Müller, P., Olbers, D.J., Richter, K., Sell, W., Walden, H., 1973. Measurements of wind-wave growth and swell decay during the Joint North Sea Wave Project (JONSWAP). Ergänzungsheft zur Deutschen Hydrographischen Zeitschrift, Reihe A(8), vol. 12, p. 95.

Hasselmann, S., Hasselmann, K., Allender, J.H., Barnett, T.P., 1985. Computations and parameterizations of the nonlinear energy transfer in a gravity-wave spectrum, part II: parameterizations of the nonlinear energy transfer for application in wave models. J. Phys. Oceanogr. 15, 1378–1391.

Hersbach, H., Janssen, P.A.E.M., 1999. Improvement of the short fetch behavior in the wave ocean model (WAM). J. Atmos. Oceanic Tech. 16, 884–892.

Hersbach, H., Janssen, P.A.E.M., 2001. Reply to comments on "improvement of the short fetch behavior in the wave ocean model (WAM)". J. Atmos. Oceanic Tech. 18, 716–721.

Herterich, K., Hasselmann, K., 1980. A similarity relation for the nonlinear energy transfer in a finite-depth gravity-wave spectrum. J. Fluid Mech. 97, 215–224.

Jenkins, A., Phillips, O.M., 2001. A simple formula for nonlinear wave–wave interactions. Int. J. Offshore Polar Eng. 11, 81–86.

Komatsu, K., Masuda, A., 1996. A new scheme of nonlinear energy transfer among wind waves: RIAM method – algorithm and performance. J. Oceanogr. 52, 509–537.

Krasnopolsky, V.M., Fox-Rabinovitz, M.S., Tolman, H.L., Belochitski, A.A., 2008. Neural network approach for robust and fast calculation of physical processes in numerical environmental models: compound parameterizations with quality control of larger errors. Neural Netw. 21, 535–543.

Krasnopolsky, V.M., Schiller, H., 2003. Some neural network applications in environmental sciences part I: forward and inverse problems in geophysical remote measurements. Neural Netw. 16, 321–334.

Long, C.E., Resio, D.T., 2007. Wind wave spectral observations in Currituck Sound, North Carolina. J. Geophys. Res. 112, C05001.

Masuda, A., 1980. Nonlinear energy transfer between wind waves. J. Phys. Oceanogr. 10, 2082–2093.

Resio, D.T., Perrie, W., 1991. A numerical study of nonlinear energy fluxes due to wave-wave interactions. Part 1: Methodology and basic results. J. Fluid Mech. 223, 603–629.

Rice, S.O., 1944. Mathematical analysis of random noise. Bell System Techn. J. 23, 282–332.

SWAMP group, 1985. Ocean Wave Modelling. Plenum Press. p. 256.

Tamura, H., Waseda, T., Miyazawa, Y., Komatsu, K., 2008. Current-induced modulation of the ocean wave spectrum and the role of nonlinear energy transfer. J. Phys. Oceanogr. 38, 2262–2684.

Tolman, H.L., 1992. Effects of numerics on the physics in a third-generation wind–wave model. J. Phys. Oceanogr. 22, 1095–1111.

Tolman, H.L., 2002. Limiters in third-generation wind wave models. The Global Atmos. Ocean Syst. 8, 67–83.

Tolman, H.L., 2003. Optimum Discrete Interaction Approximations for wind waves. Part 1: Mapping using inverse modeling. Tech. Note 227. NOAA/NWS/NCEP/MMAB. 57 pp. + Appendices.

Tolman, H.L., 2008. Optimum Discrete Interaction Approximations for wind waves. Part 3: Generalized Multiple DIAs. Tech. Note 269. NOAA/NWS/NCEP/MMAB. 117 pp.

Tolman, H.L.,2009a. Practical nonlinear interaction algorithms. In: 11th International Workshop on Wave Hindcasting and Forecasting & Coastal Hazards Symposium, JCOMM Tech. Rep. 52, WMO/TD-No. 1533. Paper J2.

Tolman, H.L., 2009b. User manual and system documentation of WAVEWATCH III™ version 3.14. Tech. Note 276. NOAA/NWS/NCEP/MMAB. 194 pp. + Appendices.

Tolman, H.L., 2010. Optimum Discrete Interaction Approximations for wind waves.Part 4: Parameter optimization. Tech. Note 288. NOAA/NWS/NCEP/MMAB. 175 pp.

Tolman, H.L., Balasubramaniyan, B., Burroughs, L.D., Chalikov, D.V., Chao, Y.Y., Chen, H.S., Gerald, V.M., 2002. Development and implementation of wind generated ocean surface wave models at NCEP. Wea. Forecasting 17, 311–333.

Tolman, H.L., Krasnopolsky, V.M., 2004. Nonlinear interactions in practical wind wave models. In: Eighth International Workshop on Wave Hindcasting and Forecasting, JCOMM Tech. Rep. 29, WMO/TD-No. 1319. Paper E1.

Tolman, H.L., Krasnopolsky, V.M., Chalikov, D.V., 2005. Neural Network approximations for nonlinear interactions in wind wave spectra: direct mapping for wind seas in deep water. Ocean Mod. 8, 178–253.

Tracy, B., Resio, D.T., 1982. Theory and calculation of the nonlinear energy transfer between sea waves in deep water. WES Report 11. US Army Corps of Engineers.

Van Vledder, G.P., 2000. Improved method for obtaining the integration space for the computation of nonlinear quadruplet wave-wave interaction. In: Proceedings of the Sixth International Workshop on Wave Forecasting and Hindcasting, pp. 418–431.

Van Vledder, G.P., 2006. The WRT method for the computation of non-linear four wave interactions in discrete spectral wave models. Coastal Eng. 53, 223–242.

Van Vledder, G.P., Herbers, T.H.C., Jenssen, R.E., Resio, D.T., Tracy, B., 2000. Modelling of non-linear quadruplet wave-wave interactions in operational wave models. In: Proceedings of 27th International Conference on Coastal Engineering, Sydney, Australia, ASCE. pp. 797–811.

Wahle, K., Günther, H., Schiller, H., 2009. Neural network parameterisation of the mapping of wave spectra onto nonlinear four-wave interactions. Ocean Mod. 30, 48–55.

WAMDIG, 1988. The WAM model – a third generation ocean wave prediction model. J. Phys. Oceanogr. 18, 1775–1810.

Webb, D.J., 1978. Non-linear transfers between sea waves. Deep-Sea Res. 25, 279–298.

Young, I.R., Van Vledder, G.P., 1993. A review of the central role of nonlinear interactions in wind–wave evolution. Trans. Roy. Soc. London 342, 505–524.

Zakharov, V.E., Pushkarev, A.N., 1999. Diffusion model of interacting gravity waves on the surface of deep fluid. Nonlinear Proc. Geoph. 6, 1–10.